Environmental Engineering and Management Journal

January 2021, Vol. 20, No. 1, 43-52
http://www.eemj.icpm.tuiasi.ro/; http://www.eemj.eu

"Gheorghe Asachi" Technical University of Iasi, Romania

ECO-FRIENDLY SYNTHESIS OF SILVER NANOPARTRICLES USING *Gazania rigens* AND EVALUATION OF ACTIVITIES

Tayyaba Shahzadi*, Amina Kanwal, Hifzah Jabeen, Tauheeda Riaz, Maria Zaib

Department of Chemistry, Government College for Women University, Sialkot-51310, Pakistan

Abstract

The present study describes the facile synthesis of silver nanoparticles (AgNPs) by green method using aqueous extract of *Gazania rigens*. The size, morphological, compositional and optical properties of silver nanoparticles were examined through X-ray diffraction (XRD), Energy Dispersive X-ray spectroscopy (EDX), Scanning Electron Microscope (SEM), and UV-Vis spectroscopy respectively. Ultraviolet-Visible spectra showed the absorbance band between 425–460 nm which indicated the synthesis of stable AgNPs. Average size of AgNPs was calculated from XRD spectra as 31.35 nm. SEM and EDX spectra confirmed the synthesis of spherical shaped AgNPs. FTIR spectra showed that different functional groups were present in aqueous extract of plant which acted as reducing agents in the formation of stable silver nanoparticles. The value of DPPH radical inhibition by AgNPs was 75.45±1.12% at 1000 µg/mL concentration revealing its moderate antioxidant activity. Synthesized AgNPs showed good total phenolic contents (262.60±1.2 mg/g GAE) as well as good total antioxidant activity (1.11±0.07). Then the synthesized AgNPs were used as catalyst for the removal of toxic organic dyes i.e methylene blue (MB) and congo red (CR). Various factors like temperature, pH, adsorbent dosage, dye concentration and contact time were examined and optimized for maximum removal of dyes. Thermodynamic factors like enthalpy (ΔH^o), Gibb's free energy (ΔG^o), and entropy (ΔS^o) of the system were also determined. Kinetics of the system was studied with the help of Lagergren's model. Adsorption parameters were also calculated using Langmuir and Freundlich, isotherm models.

Keywords: congo red, *Gazania rigens*, kinetic, methylene blue, thermodynamic

Received: December, 2019; Revised final: July, 2020; Accepted: July, 2020; Published in final edited form: January, 2021

1. Introduction

Now a day's nanotechnology has been raised as essential discipline of research. Nanotechnology deals with nanometer sized objects. Several materials, systems and devices have been developed using this technology. Nanoparticles are studied due to their distinctive physical and chemical properties, which is size dependent (Matei et al., 2016; Saruchi et al., 2019; Xu et al., 2014). Various physical and chemical methods for synthesis of nanoparticles have been reported but chemical and physical methods are being replaced by green synthesis techniques to avoid utilization of lethal solvents, high energy utilization, and dangerous by products etc (Rai and Yadav, 2013). Synthesis of nanoparticles from plants have gained popularity due to its low cost and eco-friendly nature. Thus numerous individuals have prepared nano-particles by utilizing extracts from different plant's parts like leaves, stem and flowers along with other natural products (Ravindran et al., 2013). In the scientific community silver nanoparticles have great interest due to their extensive range of applications. For the cancer diagnosis and treatment, silver nanoparticles are effectively used (Ahmed S. et al., 2016). Furthermore green synthesized AgNPs have various applications in drug delivery, gene therapy and for bio-labeling. AgNPs are very beneficial as optical receptors, reagents in chemical reactions, intercalation material for solar energy batteries,

* Author to whom all correspondence should be addressed: e-mail: tayyaba332@gmail.com; tayyaba.shehzadi@gcwus.edu.pk; Phone: (+92)-52-9250170

careful coatings for solar energy absorption and as antimicrobial, antifungal and antioxidant agents (Sopan and Vijay, 2016). Silver is nontoxic for human cells in small amounts, however fatal for most of the bacteria and viruses and henceforth widely utilized in sterilization of water and food in daily life. Plant extract is used as reducing agent to synthesize metallic NPs. The metal ions are reduced and nucleation of reduced metal atoms takes place. Then the small nearby NPs are associated and larger size particles are formed that exhibit greater thermodynamic stability (Nasrollahzadeh and Sajadi, 2015).

Gazania rigens belongs to the family Asteraceae. It is a flowering plant that is cultivated on a huge scale in gardens and landscapes (Foroutan et al., 2015). *Gazania* is utilized in medicine in order to inhibit miscarriage and tooth aching. It is also assimilated in cleansing measures particularly with aloes. Some studies have revealed the biotic effects of *Gazania* that explain its hepatoprotective and antioxidant activity (Elkhayat et al., 2016). *Gazania rigens* contains various flavonoids (luteolin, apigenin, apigenin 7-*O*-*β*-D-glucopyranosid, luteolin 7-*O*-*β*-D-glucopyranosid) and phenolic acids (chlorogenic acid, caffeic acid and 3,5-di-*O*-caffeoylquinic acid) (Desoukey et al., 2016) which are responsible for the reduction of metal ions.

In the current study, spherical shaped AgNPs were successfully synthesized by a simple and low cost method by aqueous extract of *Gazania rigens*. The obtained AgNPs were characterized by UV-Vis spectroscopy, XRD, EDX and SEM followed by its *in vitro* antioxidant activity. Furthermore adsorption experiments were performed for the removal of MB and CR dye to assess its catalytic behavior.

2. Material and methods

2.1. Preparation of plant extract

Fresh plant of *Gazania rigens* was washed thoroughly with distilled water to remove dirt and other contaminations. Then plant was dried under shade and crushed into fine powder. Then 1.5 g of the whole plant powder was taken in a beaker containing 100 ml of distilled water followed by heating on the hot plate at 80ºC for 60 minutes, the color of mixture turned yellow. The extract was then allowed to cool at room temperature and then it was filtered by using Whatt's man filter paper. This filtrate was stored in refrigerator for further studies (Modi et al., 2015).

2.2. Synthesis of Ag nanoparticles

To prepare Ag nanoparticles, 80 mL of aqueous extract of *Gazania rigens* was added to 400 ml of 0.03 molar silver nitrate solution at room temperature with constant stirring for 20 min. Silver ions (Ag^+) were reduced to Ag^0 by phytochemical constituents present in aqueous extract, color of reaction mixture was changed that indicated the synthesis of Ag nanoparticles (Sopan and Vijay, 2016). Then this colored solution of Ag nanoparticles was centrifuged at 3000 rpm for 30 min to separate AgNPs (Moodley et al., 2018).

2.3. Characterization of Ag nanoparticles

UV-Visible spectra was recorded on a UV/Vis spectrophotometer (Mettler-Toledo, UV 5) which monitored the reduction of silver ions by aqueous extract of *Gazania rigens.* The molecular structure of silver nanoparticles was determined by using X-ray diffraction (JEOL, Neoscope, JCM-600). The surface morphology and elemental composition of green synthesized AgNPs were analyzed by Scanning Electron Microscope and Energy-Dispersive X-ray spectroscopy (JEOL, Neoscope, JCM-600) respectively. FTIR spectra of the aqueous extract of *Gazania rigens* plant was recorded by using Fourier Transform Infrared spectroscopy (Agilent Technologies) to get information relating to chemical bonds.

2.4. Antioxidant activity

- *DPPH radical scavenging activity*

By using 2, 2-diphenyl-1-picrylhydrazyl hydroxyl radical (DPPH), scavenging activity of nanoparticles was assessed according to cited method (Lee and Shibamoto, 2001).

- *Total phenolic contents*

Total phenolic contents were checked by standard method (Makkar et al., 1993).

- *Phosphomolybdenum complex method*

The antioxidant activity of synthesized silver nanoparticles was checked by reported method (Prieto et al., 1999).

2.5. Dyes adsorption studies

For degradation of methylene blue and congo red dyes, stock solutions of 1000 ppm concentrations were prepared. Various working solutions (5 ppm, 10 ppm, 25 ppm, 75 ppm and 100 ppm) were made from that stock solution for the dye removal studies. Different factors like time, pH, and adsorbent concentration, effect of dye concentration and effect of temperature were optimized for maximum removal of dyes.

3. Results and discussion

3.1. Characterization of silver nanoparticles

UV–Visible spectral analysis confirmed the formation of AgNPs using 3 mM solution of $AgNO_3$ along with plant extract. UV–Vis spectrum (Fig. 1) of the reaction media was taken at different time intervals. It was observed that by increasing the time of reaction there was no change in λ_{max} but peaks become sharp. The UV–Vis absorption band in range

of 425–460 nm confirmed the presence of surface plasmon resonance of AgNPs (Ankamwar et al., 2005; Saxena et al., 2010).

In the entire XRD spectrum of green synthesized silver nanoparticles (Fig. 2), four intense peaks were observed with 2θ values 28.06º, 32.51º, 38.37º and 46.50º respectively. The XRD spectrum was compared with the standard powder diffraction card of JCPDS, silver file No. 04-0783. Peak at 28.06º and 38.37º indicated the presence of silver metal. While the peaks at 32.51º and 46.50º is due to presence of $AgNO_3$ which might have not been reduced and remain in sample as impurity (Krithiga et al., 2015; Mehta et al., 2017). XRD pattern thus evidently elucidated that the AgNPs were synthesized with average size of 31.35 nm (Hosokawa et al., 2007). The size of AgNPs was calculated by utilizing Debye-Scherer Eq. (1).

$$D = \frac{k\lambda}{\beta \cos\theta} \quad (1)$$

where D denotes the average particle size of nanoparticles in nm, β is full width at half maximum (FWHM) of the diffraction peak, K is the Scherrer constant with the value of 0.9-1, λ is the wavelength of the X-ray (0.15406 nm), θ is Bragg angle (θ=2θ/2).

SEM spectra (Figs. 3a-d) elucidated that AgNPs had roughly spherical shape and homogenously distributed all over the surface. Some of AgNPs might be present in agglomeration. So, SEM micrographs showed the agglomeration of nanoparticles and nanoclusters in its topical view (Ahmed K. et al., 2016).

The EDX spectrum (Fig. 4) showed prominent peaks of silver at voltage from 2.5 to 3.5 KeV and confirmed the formation of Ag nanoparticles (Gomathi et al., 2017). These peaks assigned to the silver characteristic of K and L lines. Maximum peak on the left side of spectrum at value of 0.2 KeV indicated the presence of carbon. While peak at 0.5 KeV indicated the presence of oxygen characteristic line. The carbon and oxygen signal was due to presence of adsorbed biomolecules coated over the surface of silver nanoparticles (Puchalski et al., 2007).

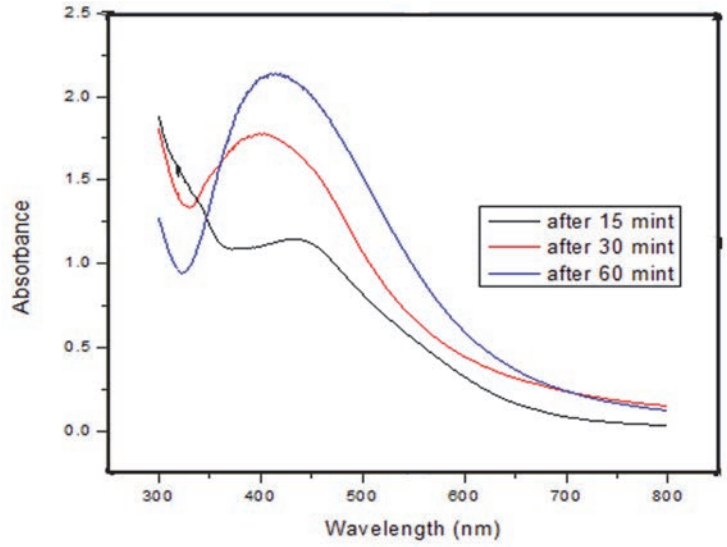

Fig. 1. UV-Vis spectrum of synthesized AgNPs

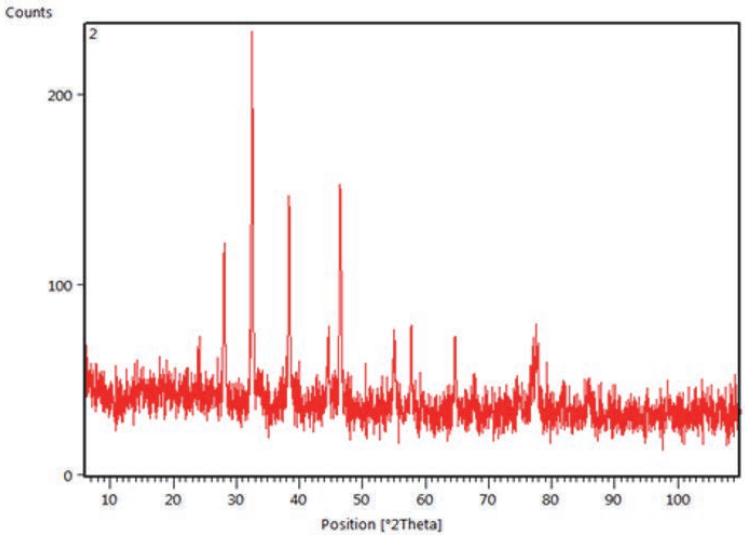

Fig. 2. XRD spectrum of synthesized AgNPs

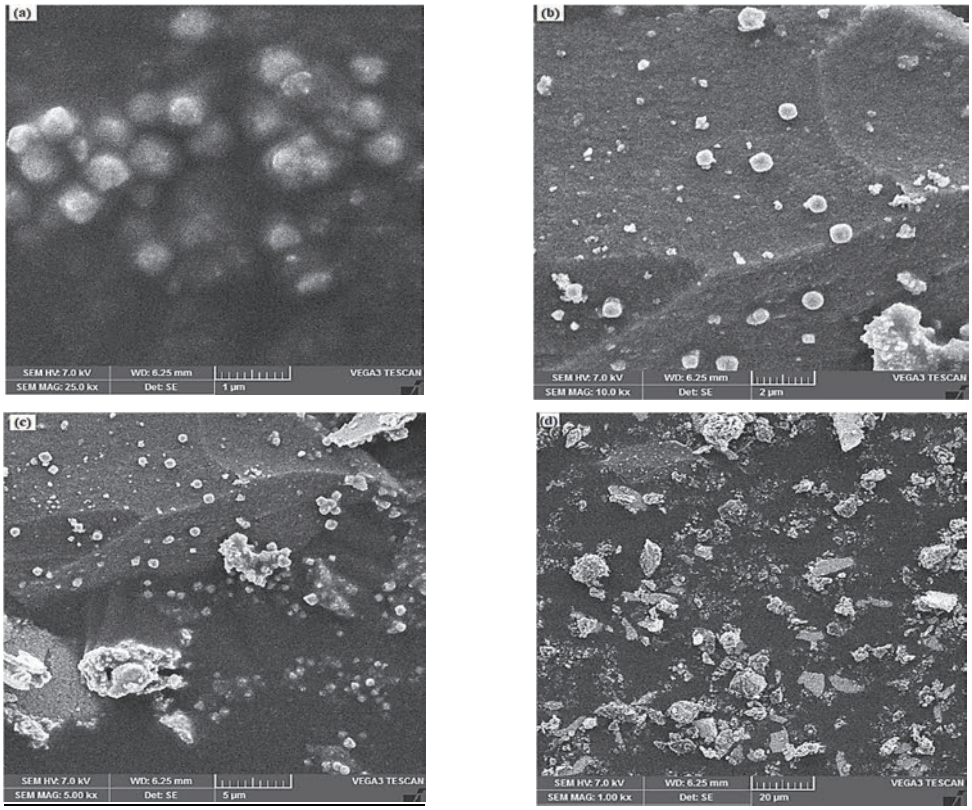

Fig. 3. SEM spectra of synthesized AgNPs: (a) at 1 µm, (b) at 2 µm, (c) at 5 µm, (d) at 20 µm

FTIR spectrum of aqueous extract of *Gazania rigens* has been shown in Fig. 5. FTIR measurements depicted the functional moieties of possible biomolecules involved in reduction and efficient stabilization of metal nanoparticles synthesized by aqueous extract of *Gazania rigens*.

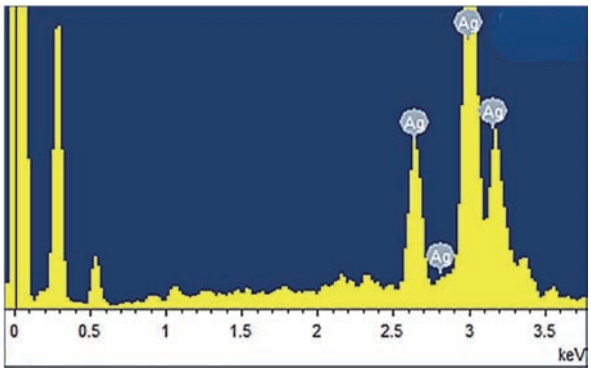

Fig. 4. EDX spectrum of synthesized AgNPs

Band at 3200 cm^{-1} corresponds to the O-H stretching, indicating presence of alcohols and phenols. Band at 1628 cm^{-1} and 1484 cm^{-1} can be attributed to asymmetric and symmetric stretch of carboxylate group. Absorption bands at 1134 cm^{-1} and 1000 cm^{-1} are due to C-O stretching in esters and alcohols respectively (Banerjee et al., 2014; Prathna et al., 2011). Literature studies revealed the presence of carbohydrates, flavonoids, and phenolic compounds in *Gazania rigens*. Possible mechanism for the reduction of Ag^{+} to Ag^{0} and formation of stable silver nanoparticles by the phytoconstituents present in aqueous extract of *Gazania rigens* has been given in Fig. 6.

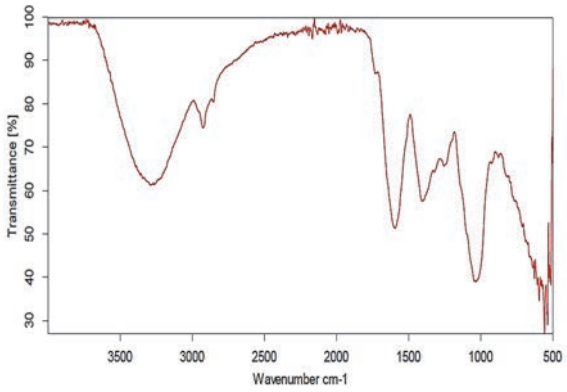

Fig. 5. FTIR spectrum of aqueous extract of *Gazania rigens*

3.2. Antioxidant assays

3.2.1. DPPH radical scavenging activity

DPPH is a stable radical that was utilized to evaluate radical scavenging activity of the samples. Any material that has the ability to donate an electron or hydrogen atom to the DPPH radical, reduces it to form a stable diamagnetic molecule (Hasan et al., 2009). By comparison with butylated hydroxyl toluene (BHT) a reference antioxidant, the DPPH radical scavenging activity of different concentrations of the AgNPs was measured and it was revealed that scavenging activity increased in a dose dependent mode as given in Table 1.

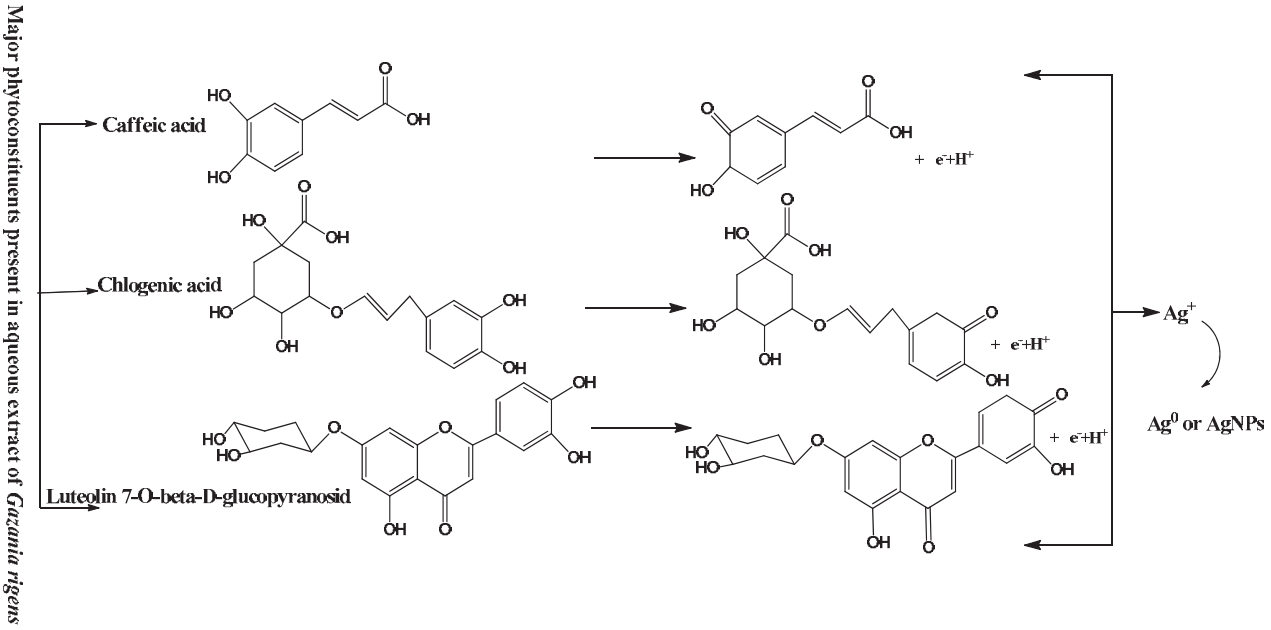

Fig. 6. Possible mechanism for reduction of $AgNO_3$ to AgNPs by the phytoconstituents present in aqueous extract of *Gazania rigens*

3.2.2. Total phenolic contents

This method was used to check antioxidant activity by inhibition of free radicals formed by the decay of hydroperoxides. They also protect against pathogens and predators by forming metal chelate ions.

The total phenolic contents of synthesized AgNPs were spectrophotometrically assessed by using Follin-Ciocalteu´s reagent at 725 nm (Skerget et al., 2005). Total phenolic contents of AgNPs were found good (262.60 ± 1.2 GAE mg/g) as compared to blank shown in Table 2.

3.2.3. Phosphomolybdenum complex method

This method was also used to check total antioxidant activity of the synthesized nanoparticles. In this method at acidic pH green phosphate Mo (V) complex is formed because antioxidants reduced molybdenum (VI) to molybdenum (V). Generally this method detects antioxidants, like carotenoids, ascorbic acid, tocopherols and some phenolics (El Hajaji et al., 2010). By comparing with BHT the total antioxidant activity of the AgNPs was calculated and its value was found to be very good i.e 1.11±0.07 as shown in Table 1-b.

3.3. Dyes adsorption studies

3.3.1. Effect of adsorbent dosage

To study the influence of adsorbent dosage a graph was plotted against dye removal (%) utilizing AgNPs at fixed initial dye concentration. Influence of adsorbent dosage was examined by keeping all the experimental factors (C_{dye} = 5 mg/L, V= 25 mL) constant and varying the adsorbent amount (5 mg, 10 mg, 25 mg, 75 mg and 100 mg). As the concentration of adsorbent was increased the efficiency of dye removal was also increased up to a certain level of adsorbent dosage and after that the dye removal efficiency become constant (Fig. 7a).

Table 1. DPPH radical scavenging activity of synthesized AgNPs

Sr. No.	*Sample*	*Concentration in Assay (µg/mL)*	*% Scavenging of DPPH radical ± S.E.M*
1	AgNPs	1000	75.45± 1.12
		500	58.92 ± 0.8
		250	40.73± 0.34
2	BHT	60	94.35 ± 0.14
		30	78.46 ± 0.08
		15	46.57 ± 0.05

Table 2. Total phenolic contents and total antioxidant activity of synthesized AgNPs

Sr. No.	*Sample*	*Total phenolics (GAE, mg/g)*	*Total antioxidant activity*
1	AgNPs	262.60±1.2	1.11±0.07
2	BHT	-	0.85±1.22
3	Blank	11.98	-

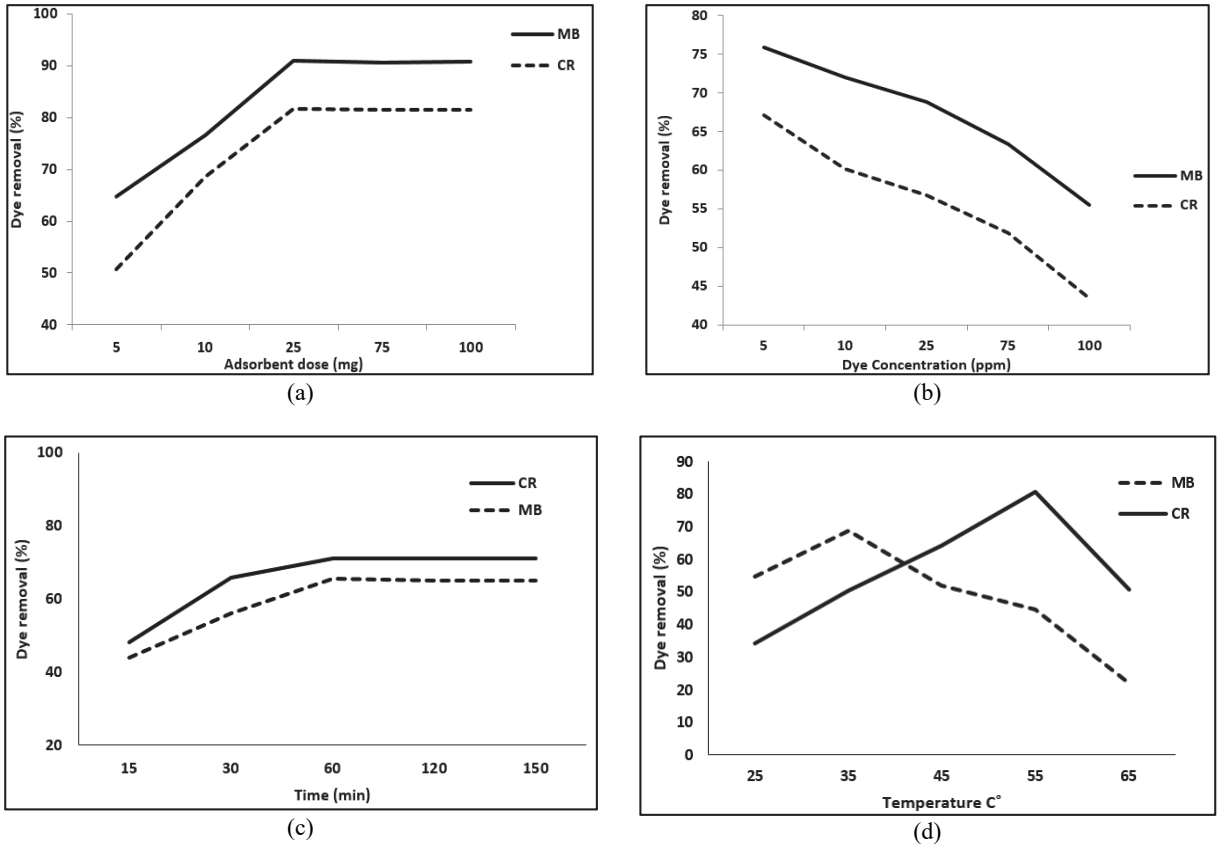

Fig. 7. (a) Effect of adsorbent dosage on removal (%) of CR and MB; (b) Effect of dye concentration on removal (%) of CR and MB dye by AgNPs; (c) Effect of contact time on % removal of CR and MB dye by AgNPs; (d) Effect of temperature on % removal of CR and MB dye by AgNPs

In both MB and CR dyes, with increase in adsorbent dosage percentage removal was increased but it become constant at 25 mg of adsorbent dosage and by further increase in adsorbent dosage, there was no effect on dye removal. It may be due to the fact that by increasing adsorbent dosage the numbers of accessible surface active sites became greater and equilibrium was attained to certain extent because of the agglomeration of the surface active sites (Garg et al., 2004). However maximum removal was attained in case of MB i.e 90 % in comparison to CR i.e 81 % at 25 mg of adsorbent dosage.

3.3.2. Effect of dye concentration

Effect of dye concentration was studied at 10 mg fixed dosage of adsorbent and varying dye concentration (5 ppm, 10 ppm, 25 ppm, 75 ppm and 100 ppm, V=25 mL). In both MB and CR dyes with increase in dye concentration, the % age removal by AgNPs was decreased (Fig. 7b). At dye concentration (10 mg/mL), the removal efficiency of AgNPs was 75.9% and 67% for MB dye and CR dye, respectively.

Fig. 7b shows that % removal reduced with increasing preliminary dye concentration from 5 ppm to 100 ppm. Maximum removal occurred at 5 ppm of dye concentration because of the greater number of active sites available on the surface of AgNPs. Conversely, at higher concentration of dye, saturation of binding sites occurred that reduced the active reaction sites and might resulted in decrease in the adsorption efficiency (Rehman et al., 2013).

3.3.3. Effect of time

To check effect of time on the dye removal efficiency by AgNPs, experiment was carried out using dye concentration (C_{dye}=5 mg/L, V=25 mL) and 10 mg of adsorbent dosage with interaction time ranging from 10 to 150 minutes. The dye removal (%) was constantly increased from 48 to 71% and 43 to 65% with increasing the interaction time from 10 to 150 minutes for MB dye and CR dye, correspondingly (Fig. 7c).

It was observed that initially there was rapid increase in dye removal efficiency due to larger number of available reaction sites on the surface of AgNPs and after some time removal efficiency becomes constant when equilibrium was established between dye molecules and surface active sites of AgNPs (Saad et al., 2017). Comparative study showed that both dyes have same trend but MB exhibited slightly higher dye removal efficiency as compared to CR.

3.3.4. Effect of temperature

The influence of temperature on the removal (%) of CR and MB (C_{dye}=5 mgL^{-1}; V=25 mL by 10 mg of AgNPs was studied at different temperature range (25°C, 35°C, 45°C, 55°C and 65°C) (Fig. 7d). The figure showed that initially, removal of dyes increased with increase in temperature as elevated temperature leads to faster mobility and rapid penetration of dyes

molecules (adsorbate) into the pores of the nanoparticles (adsorbent).

However after a certain temperature limit, escaping ability of dye molecules also increased with increase in temperature leading to less adsorption capacity (Xia et al., 2019). Another reason, removal percentage of dye increased with the increasing temperature to a limit, as further increase in temperature, removal efficiency decreased because of physical bonding among dye molecules and the active sites of adsorbent surface weaken with increasing temperature (Hu et al., 2010). The maximum temperature for dyes removal was 35°C and 55°C for CR dye and MB dye, respectively.

3.3.5. Effect of pH

The influence of pH on MB and CR dyes (C_{dye}= 5 mg L^{-1}, V=25 mL) removal was examined in range of 2-12 pH by using 10 mg of adsorbent dosage. For CR dye the maximum removal (%) was observed in acidic media at pH 4 (Fig. 8).

By increasing the pH above 4, CR removal was decreased constantly. The reason of this phenomenon may be due to the proliferation in electrostatic repulsion among negatively charged (OH^{-1}) surface of the AgNPs and negatively charged molecules of dye (Dawood and Sen, 2012). As the molecules of MB dye were positively charged, so at lower pH value electrostatic repulsion among the positively charged surface of the AgNPs and MB dye molecules was greater that indicated the lesser dye removal. Dye removal increased constantly by increasing the pH. After pH 8.0 there was no significant removal of dye. The maximum removal of MB dye was observed at pH 8.0.

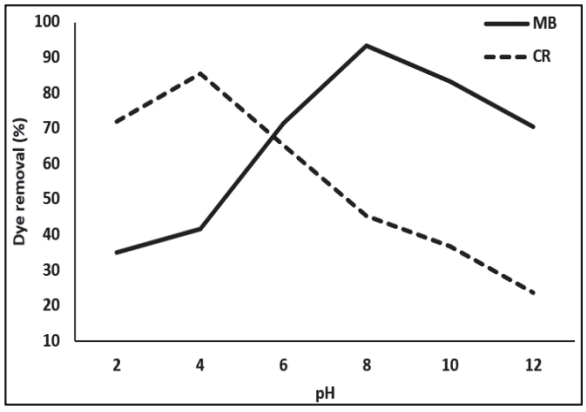

Fig. 8. Effect of pH on % removal of CR and MB dye by AgNPs

3.4. Thermodynamic study

The thermodynamic parameters ΔG^o, ΔS^o and ΔH^o was calculated by using the following Eqs. (2-4):

$$\ln Kd = \frac{\Delta H^0}{RT} - \frac{\Delta S}{R} \quad (2)$$

$$Kd = \frac{C_0}{C_e} \quad (3)$$

$$\Delta G^0 = -RT \ln K_d \quad (4)$$

Van't Hoff equation (2) was used to determine standard enthalpy change ΔH^o and standard entropy change ΔS^o. To calculate the thermodynamic parameters graph was plotted between *lnKd* and *1/T* (Fig. 9). From slope value of ΔH^o and from intercept value of ΔS^o was calculated. Then by using Eq. (4), ΔG^o value was determined. For both dyes the value of ΔG^o was negative which showed their spontaneous behavior. Whereas the value of ΔH^o for MB is positive and for CR is negative that indicates the reaction was endothermic and exothermic, respectively. The results are given in Table 3.

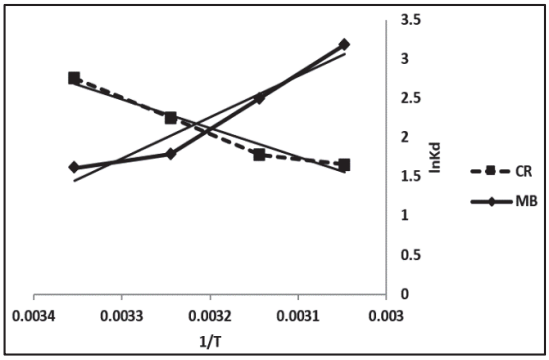

Fig. 9. Van't Hoff plots for CR and MB dye adsorption on synthesized AgNPs

3.5. Kinetic study

Kinetics information can provide knowledge on rate of dye removal process. Kinetic study was based on the Pseudo-first order as it can be seen from Fig. 9. Lagergren's pseudo first order Eq. (5) was used for kinetic study (Bellu et al., 2010).

$$log(q_e - q_t) = log\, q_e \quad (\frac{k_1}{2.303})t \quad (5)$$

Here q_e denotes the adsorption capability at equilibrium time and q_t at time *t*. Kinetic rate constant was denoted with k_1 (min^{-1}). The graph was plotted between *log (qe-qt)* and *t* (Fig. 10) and value of rate constant was calculated from the slope as given in Table 4.

3.6. Adsorption isotherm

Freundlich and Langmuir adsorption models were used to study the adsorption behaviour of MB and CR on AgNPs.

3.6.1. Freundlich adsorption Isotherm

Freundlich isotherm explains the multilayer adsorption process is localized to a heterogeneous surface.

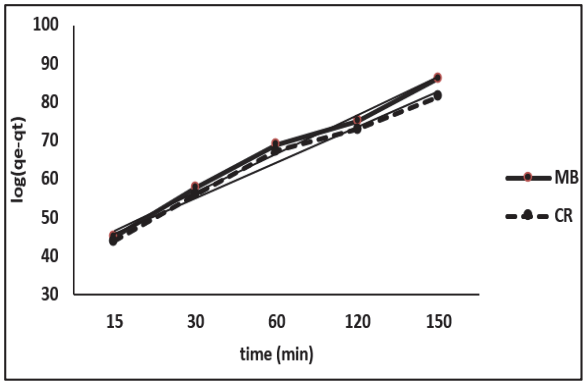

Fig. 10. Pseudo 1st order reaction of MB and CR adsorption on AgNPs

Freundlich isotherms models can be represented by below (Eq. 6):

$$\log \frac{x}{m} = \log K + \frac{1}{n} \log C_e \quad (6)$$

where *x/m* is the amount adsorbed per unit mass of adsorbent. *Ce* is the equilibrium concentration and *1/n* and *K* are Freundlich constants (Vijayakumar et al., 2012).

The resulting plots for MB and CR were shown in Fig. 11. Value of *1/n* show the type of isotherm to be favorable (*1/n* lower than 1), irreversible (*1/n* = 0) and unfavorable (*1/n* higher than 1). The value of *n* should be less than 10 and higher than unity for favorable adsorption conditions. The values of Freundlich constant *n* were more than 1 for both dyes, indicate that the adsorption process is favorable (Table 4).

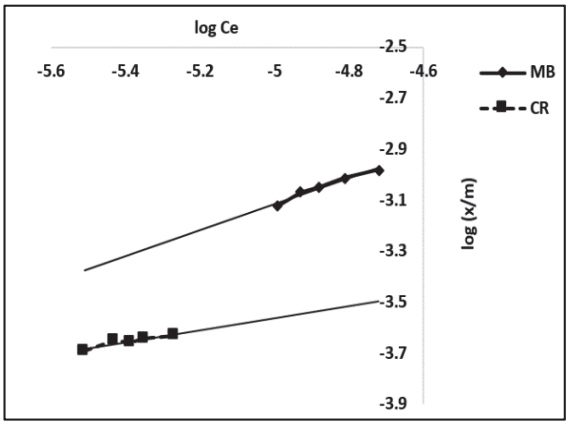

Fig. 11. Freundlich Isotherm for MB and CR adsorption on AgNPs

3.6.2. Langmuir adsorption isotherm

In the Langmuir model, the adsorbent surface is homogeneous, therefore adsorption occurs on a monolayer in all adsorption sites (Mantosh et al., 2013). The Langmuir isotherm Eq. (7) is expressed as:

$$\left(\frac{C_e}{x/m}\right) = \left(\frac{1}{KV_m}\right) + \left(\frac{C_e}{V_m}\right) \quad (7)$$

where *Vm* and *K* represent Langmuir constants. The constant *Vm* is the monolayer capacity and *K* gives a measure of adsorbing capacity and shows the nature of binding.

The Langmuir isotherm for both dyes adsorption on ZnO NPs are shown in Fig. 12. Langmuir isotherm separation factor (R_L) is used to evaluate the adsorption feasibility. It is calculated using Eq. (8):

$$R_L = \frac{1}{1+(1+KC_0)} \quad (8)$$

From Langmuir constant we can find the value of *R*. C_0 is initial concentration *K* = the constant related to the energy of adsorption (Langmuir Constant). R_L value indicates the adsorption nature to be either unfavourable if R_L>1), linear if R_L =1, favourable if 0< R_L<1 it means adsorption is irreversible.

For both dyes adsorption onto nanoparticle, the value of R is less than 1 and greater than zero so it shows that adsorption is favourable and it follows Langmuir adsorption isotherm. Maximum monolayer capacity was calculated by using Langmuir adsorption model and is given in Table 5.

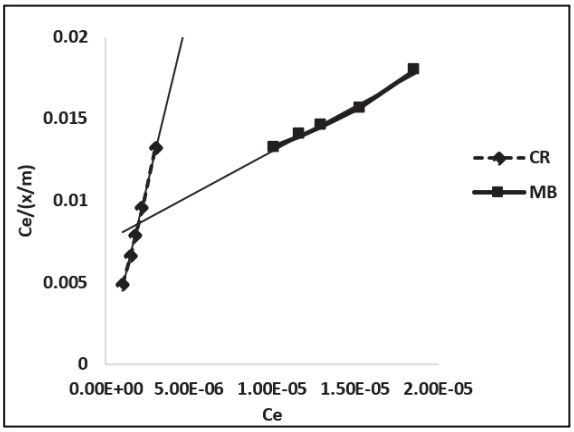

Fig. 12. Langmuir isotherm for MB and CR adsorption on AgNPs

4. Conclusion

It was concluded that AgNPs successfully synthesized by eco-friendly single step procedure, with aqueous extract of *Gazania rigens* and characterized by UV-visible spectra, XRD, SEM, EDX and FTIR measurements.

The synthesized AgNPs had significant total antioxidant activity, total phenolic contents and moderate value of DPPH scavenging activity which was increased by increasing adsorbent dosage. Various factors like temperature, pH, adsorbent dosage, dye concentration and contact time were optimized for maximum removal of dyes by synthesized AgNPs. Thermodynamic studies showed that removal of dyes was a spontaneous behavior and their kinetic study indicated that it was pseudo first order.

Table 3. Thermodynamic parameters for removal of CR and MB dye by AgNPs

Temp. (K)	*Congo Red (CR) dye*			*Methylene Blue (MB) dye*		
	ΔG^0 (KJmol^{-1})	ΔS^0 (Jmol^{-1}K^{-1})	ΔH^0 (KJmol^{-1})	ΔG^0 (KJmol^{-1})	ΔS^0 (Jmol^{-1}K^{-1})	ΔH^0 (KJmol^{-1})
298	-6.829	-80.6541	-30.718	-4.002	159.155	43.857
308	-5.779			-4.593		
318	-4.699			-6.637		
328	-4.539			-8.689		

Table 4. Kinetic Rate constant (min^{-1}) for MB and CR dye adsorption on AgNPs

Kinetic model	*Factors*	*Values of both dyes*	
		MB	*CR*
Pseudo first order	K_1 (min$^{-1)}$	21.2055	82.29
	q_e (cal)	3.496	3.603
	R^2	0.980	0.988

Table 5. Freundlich and Langmuir isothermal model for the adsorption of MB and CR on AgNPs

Dye	*Freundlich parameters*			*Langmuir parameters*		
	Log K	*1/n*	R^2	*Adsorption capacity (K)*	*Monolayer capacity V_m(mg/g)*	R^2
Methylene blue	-0.5733	0.508	0.97	72328	1.81	0.987
Congo red	-2.3733	0.2375	0.86	8434.00	2.30	0.998

The adsorption studies confirmed that the adsorption process of MB and CR on AgNPs followed the Freundlich and Langmuir model. Overall the studied green method for the synthesis of AgNPs was found to be environmentally safe as no additional surfactants or reductants were needed for the stabilization of AgNPs.

Furthermore synthesized silver nanoparticles had potential to be used in pharmacological preparations as well as they also exhibit excellent catalytic activity for the adsorption of dyes.

References

Ahmed S., Ahmad M., Swami B.L., Ikram S., (2016), A review on plants extract mediated synthesis of silver nanoparticles for antimicrobial applications a green expertise, *Journal of Advanced Research*, **7**, 17-28.

Ahmed K., Tariq I., Siddiqui S.U., Mudassir M., (2016), Green synthesis of cobalt nanoparticles by using methanol extract of plant leaf as reducing agent, *Pure and Applied Biology*, **5**, 453-457.

Ankamwar B., Damle C., Ahmad A., Sastry M., (2005), Biosynthesis of gold and silver nanoparticles using *Emblica officinalis* fruit extract their phase transfer and transmetallation in an organic solution, *Journal of Nanoscience and Nanotechnology*, **5**, 1665-1671.

Banerjee P., Satapathy M., Mukhopahayay A., Das P., (2014), Leaf extract mediated green synthesis of silver nanoparticles from widely available Indian plants synthesis characterization antimicrobial property and toxicity analysis, *Bioresources and Bioprocessing*, **1**, 1-10.

Bellu S., Sala L., González J., García S., Frascaroli M., Blanes P., Harada M., (2010), Thermodynamic and dynamic of chromium biosorption by Pectic and lignocellulocic biowastes, *Journal of Water Resource and Protection*, **2**, 888-897.

Dawood S., Sen T.K., (2012), Removal of anionic dye Congo red from aqueous solution by raw pine and acid-treated pine cone powder as adsorbent equilibrium thermodynamic, kinetics, mechanism and process design, *Water Research*, **46**, 1933-1946.

Desoukey S.Y., EI Kady W.M., Salama A.A., Hagag E.G., EI-Shenawy S.M., EI-Shanawany M.A., (2016), Hepatoprotection and Antioxidant Activity of *Gazania longiscapa and G. rigens* with the isolation and quantitative analysis of bioactive metabolites, *International Journal of Pharmacognosy and Phytochemical Research*, **8**, 1121-1131.

El Hajaji H., Lachkar N., Alaoui K., Cherrah Y., Farah A., Ennabili A., Lachkar M., (2010), Antioxidant properties and total phenolic content of three varieties of carob tree leaves from Morocco, *Records of Natural Products*, **4**, 193-204.

Elkhayat E.S., (2016), Chemical constituents from *Gazania linearis* cultivated in Egypt, *Bulletin of Faculty of Pharmacy, Cairo University*, **54**, 257-261.

Foroutan N.A., Bahman S., Naghdi Badi H., Mehrafarin A., Labbafi M., (2015), Morpho-physiological and phytochemical traits of *Gazania rigens* affected by foliar application of bio-stimulants, *EurAsian Journal of BioSciences*, **9**, 16-21.

Garg V.K., Amita M., Kumar R., Gupta R., (2004), Basic dye methylene blue removal from simulated wastewater by adsorption using Indian Rosewood sawdust a timber industry waste, *Dyes and Pigments*, **63**, 243-250.

Gomathi M., Rajkumar P.V., Prakasam A., Ravichandran K., (2017), Green synthesis of silver nanoparticles using *Datura stramonium* leaf extract and assessment of their antibacterial activity, *Resource-Efficient Technologies*, **3**, 280-284.

Hasan S.R., Hossain M.M., Akter R., Jamila M., Mazumder M.E.H., Rahman S., (2009), DPPH free radical scavenging activity of some Bangladeshi medicinal plants, *Journal of Medicinal Plants Research*, **3**, 875-879.

Hosokawa M., Nogi K., Naito M., Yokoyama T., (2007), *Nanoparticle Technology Handbook*, 1st Edition, Elsevier Science.

Hu Z., Chen H., Ji F., Yuan S., (2010), Removal of Congo Red from aqueous solution by cattail root, *Journal of Hazardous Materials*, **173**, 292-297.

Krithiga N., Rajalakshmi A., Jayachitra A., (2015), Green synthesis of silver nanoparticles using leaf extracts of *Clitoria ternatea* and *Solanum nigrum* and study of its antibacterial effect against common nosocomial pathogens, *Journal of Nanoscience*, https://doi.org/10.1155/2015/928204.

Lee K.G., Shibamoto T., (2001), Antioxidant property of aroma extract isolated from clove buds [*Syzygium aromaticum* (L.) Merr. Et Perry], *Food Chemistry*, **74**, 443-448.

Makkar H.P., Blummel M., Borowy N.K., Becker K., (1993), Gravimetric determination of tannins and their correlations with chemical and protein precipitation methods, *Journal of the Science of Food and Agriculture*, **61**, 161-165.

Mantosh K.S., Priya B., Papita D.J., (2013), Plant-mediated synthesis of silver-nanocomposite as novel effective azo dye adsorbent, *Applied Nanoscience*, http://doi.org/10.1007/s13204-013-0286-x.

Matei E., Predescu A.M., Coman G., Balanescu M., Sohaciu M., Predescu C., Favier L., Niculescu M., (2016), Magnetic nanoparticles used in envinronmental engineering for Pb and Zn removal, *Environmental Engineering and Management Journal*, **15**, 1019-1025.

Mehta B.K., Chhajlani M., Shrivastava B.D., (2017), Green synthesis of silver nanoparticles and their characterization by XRD, *Frontiers of Physics and Plasma Science*, **836**, 012050-012054.

Modi S., Pathak B., Fulekar M.H., (2015), Microbial synthesized silver nanoparticles for decolorization and biodegradation of azo dye compound, *Journal of Environmental Nanotechnology*, **4**, 37-46.

Moodley J.S., Krishna S.B.N., Pillay K., Govender P., (2018), Green synthesis of silver nanoparticles from *Moringa oleifera* leaf extracts and its antimicrobial potential, *Advances in Natural Sciences Nanoscience and Nanotechnology*, **9**, 15-11.

Nasrollahzadeh M., Sajadi S.M., (2015), Green synthesis of copper nanoparticles using *Ginkgo biloba* L. leaf extract and their catalytic activity for the Huisgen [3+ 2] cycloaddition of azides and alkynes at room temperature, *Journal of Colloid and Interface Science*, **457**, 141-147.

Prathna T.C., Chandrasekaran N., Raichur A.M., Mukherjee A., (2011), Biomimetic synthesis of silver nanoparticles by *Citrus limon* aqueous extract and theoretical prediction of particle size, *Colloids and Surfaces B Biointerfaces*, **82**, 152-159.

Prieto P., Pineda M., Aguilar M., (1999), Spectrophotometric quantitation of antioxidant capacity through the formation of a phosphomolybdenum complex specific application to the determination of vitamin E, *Analytical Biochemistry*, **269**, 337-341.

Puchalski M., Dabrowski P., Olejniczak W., Krukowski P., Kowalczyk P., Polanski K., (2007), The study of silver nanoparticles by scanning electron microscopy, energy dispersive X-ray analysis and scanning tunnelling microscopy, *Materials Science-Poland*, **25**, 473-478.

Rai M., Yadav A., (2013), Plants as potential synthesizer of precious metal nanoparticles: progress and prospects, *IET Nanobiotechnology*, **7**, 117-124.

Ravindran A., Chandran P., Khan S.S., (2013), Biofunctionalized silver nanoparticles advances and prospects, *Colloids and Surfaces B Biointerfaces*, **105**, 342-352.

Rehman M.S.U., Munir M., Ashfaq M., Rashid N., Nazar M.F., Danish M., Han J.I., (2013), Adsorption of Brilliant Green dye from aqueous solution onto red clay, *Chemical Engineering Journal*, **228**, 54-62.

Saad M., Tahir H., Khan J., Hameed U., Saud A., (2017), Synthesis of polyaniline nanoparticles and their application for the removal of crystal violet dye by ultrasonicated adsorption process based on response surface methodology, *Ultrasonics Sonochemistry*, **34**, 600-608.

Saruchi., Thakur P., Kumar V., (2019), Kinetics and thermodynamic studies for removal of methylene blue dye by biosynthesize copper oxide nanoparticles and its antibacterial activity, *Journal of Environmental Health Science and Engineering*, **17**, 367-376.

Saxena A., Tripathi R.M., Singh R.P., (2010), Biological synthesis of silver nanoparticles by using onion extract and their antibacterial activity, *Digest Journal of Nanomaterials and Biostructures*, **5**, 427-432.

Skerget M., Kotnik P., Hadolin M., Hras A.R., Simonic M., Knez Z., (2005), Phenols, proanthocyanidins, flavones and flavonols in some plant materials and their antioxidant activities, *Food Chemistry*, **89**, 191-198.

Sopan N.K., Vijay D.M., (2016), Synthesis of silver nanoparticles using *Elephantopus scaber* leaf extract, *Materials Science and Engineering* C, **2**, 719-724.

Vijayakumar G., Tamilarasan R., Dharmendirakumar M.J., (2012), Adsorption, kinetic, equilibrium and thermodynamic studies on the removal of basic dye Rhodamine-B from aqueous solution by the use of natural adsorbent perlite, *Journal of Materials Environmental Science*, **3**, 157-170.

Xia Y., Yao Q., Zhan W., Zhang Y., Zhao M., (2019), Comparative adsorption of methylene blue by magnetic baker's yeast and EDTAD-modified magnetic baker's yeast: Equilibrium and kinetic study, *Arabian Journal of Chemistry*, **12**, 2448-2456.

Xu Y., Li C., Zhu X., Huang E.W., Zhang D., (2014), Application of magnetic nanoparticles in drinking water purification, *Environmental Engineering and Management Journal*, **13**, 2023-2029.